Developmental and Comparative Immunology 105 (2020) 103608

Contents lists available at ScienceDirect

Developmental and Comparative Immunology

journal homepage: www.elsevier.com/locate/devcompimm

The proinflammatory cytokines TNF-α and IL-6 in lumpfish (*Cyclopterus lumpus* L.) -identification, molecular characterization, phylogeny and gene expression analyses

Håvard Øritsland Eggestøl*, Harald S. Lunde, Gyri Teien Haugland**

Department of Biological Sciences, Bergen High-Technology Center, University of Bergen, PO Box 7803, NO-5020, Bergen, Norway

ARTICLE INFO

Keywords:
Proinflammatory cytokines
Lumpsucker
Tumor necrosis-factor
Interleukin
Cleaner fish
Teleost
Phylogeny
Innate immune system
Responses
PAMP
PRR
Tissue dependence
Genomic organization

ABSTRACT

The proinflammatory cytokines TNF-α and IL-6 are important mediators of inflammatory reactions and orchestrators of the immune system in vertebrate. In this study, we have identified TNF-α and IL-6 in lumpfish, molecular characterized them at mRNA and gene level, performed homology modelling and measured their gene expression in different tissues and upon *in vitro* stimulation. A comprehensive phylogenetic analysis of TNF-α teleost sequences give novel insight into the TNF –α biology. Interestingly, we identified two isoforms of luIL-6. In normal tissue and leukocyte, the level of luTNF-α transcripts was higher than luIL-6. The expression pattern were parallel, except for brain, eye and gonad, and they displayed a similar induction pattern upon exposure to PAMPs, being most highly upregulated by flagellin. This is the first in-depth characterization of TNF and IL-6 in lumpfish. In recent years, lumpfish has become an important species for the aquaculture industry and establishment of qPCR-assays of luTNF-α and luIL-6 provide a valuable tool to measure effect of immune modulation, such as vaccination, microbiological disease and physiological trials. Lumpfish is also interesting for comparative studies as it represent a phylogenetic group that is poorly described immunologically.

1. Introduction

Tumor necrosis factor alpha (TNF-α) is a pleiotropic pro-inflammatory cytokine involved in regulation of the immune response and immune system homeostasis. Also, it is a major mediator of apoptosis, cell proliferation and differentiation, and it is also involved in sleep (Dubravec et al., 1990; Krueger et al., 1998; Warner and Libby, 1989; Young et al., 1987). TNF-α is expressed as a membrane bound peptide that is enzymatically cleaved by TNF convertase (TACE), also known as ADAM17. In mice (*Mus muscelus*) the biological active peptide of TNF-α is a homotrimer with a molecular weight of 51.81 kDa. The solved crystal structures (1.4 Å resolution) of the mature murine TNF-α has revealed important receptor binding surfaces at amino acid (aa) 30–34 and 144–147 and that one 2-propanol molecule, stabilized by Tyr-119 in each monomer, is trapped inside the trimeric channel (Baeyens et al., 1999).

TNF is an ancient gene identified and characterized in several invertebrates, such as planarians, mollusks and arthropods (Hu et al., 2019; Li et al., 2017; Qu et al., 2017), as well as in vertebrate species. Among fish, TNF-α has been identified and characterized in salmonids (Bobe and Goetz, 2001; Zou et al., 2002), carp fishes (Eimon et al., 2006; Grayfer et al., 2008; Saeij et al., 2003; Savan and Sakai, 2004; Zhang et al., 2012), Japanese flounder (*Paralychthys olivaceus*) (Hirono et al., 2000), gilthead seabream (*Sparus aurata*) (Garcia-Castillo et al., 2002) as well as ayu fish (*Plecoglossus altivelis*) (Uenobe et al., 2007), bluefin tuna (*Thunnus orientalis* and *Thunnus thynnus)* (Kadowaki et al., 2009; Lepen Pleic et al., 2014), channel catfish (*Icatalarus punctatus*) (Zou et al., 2003b), tilapia (*Oreochromis niloticus*) (Praveen et al., 2006), turbot (*Scophthalmus maximus*) (Ordas et al., 2007) and rock bream (*Oplegnathus fasciatus*) (Kim et al., 2009).

Several paralogs of TNF-α have been identified in teleosts. Hong et al. (2013) divided between Type I and II, the former being structurally similar to the ancient TNF-α, while the latter type II contained a shortened pre-TACE extracellular stalk and two aa inserted between β-sheet 9 and 10. They showed that type I TNF-α is co-localized with TNF-N and gabbr1a in zebrafish, while type II TNF-α is co-localized with SCAM1L and gabbr1b. Furthermore, Hong et al. (2013) suggested that type II can be heterofunctional as the shortened stalk possibly could inhibit the TACE-action, leaving the type II in a transmembrane form.

* Corresponding author.
** Corresponding author.
E-mail addresses: Havard.Eggestol@uib.no (H.Ø. Eggestøl), Gyri.Haugland@uib.no (G.T. Haugland).

https://doi.org/10.1016/j.dci.2020.103608
Received 19 August 2019; Received in revised form 3 January 2020; Accepted 3 January 2020
Available online 07 January 2020
0145-305X/

Moreover, they also speculated that this would leave type I as mainly a secreted cytokine.

TNF-α is constitutively expressed in most examined teleost tissue. Bluefin tuna (both Pacific and Atlantic), salmonid fishes and common carp have at least two TNFα paralogs (Hong et al., 2013; Kadowaki et al., 2009; Laing et al., 2001; Lepen Pleic et al., 2014; Saeij et al., 2003; Savan and Sakai, 2004). Hong et al. (2013) observed a higher gene expression of TNF-α1 (type 1) compared to TNF-α2 (type 1) and TNF-α3 (type 2) in most examined tissues in rainbow trout. In Pacific tuna, TNF2 (type II), but not TNF1 (type I), showed a tissue dependent gene expression (Kadowaki et al., 2009). Lepen Pleic et al. (2014) did not observe any tissue dependent gene expression of the TNF-α paralogs in Atlantic tuna.

In a stimulation experiment in Pacific tuna, where head kidney leukocytes (HKLs) were exposed to various pathogen-associated molecular patterns (PAMPs), type I TNF-α did not exhibit any altered expression, while type II TNFα showed moderate upregulation by lipopolysaccharide (LPS), phytohemagglutinin, concanavalin A, pokeweed mitogen and phorbol myristate acetate (Kadowaki et al., 2009). Most examined teleost TNF-α are positively regulated by LPS. Other PAMPs also induces TNF-α levels *in vitro* in teleosts, but consensus reduction or induction patterns of non-LPS PAMPs in different species have not yet been unveiled. This is likely due to the same PAMPs is not included in the different studies. Recombinant teleost TNF-α exhibit pro-inflammatory properties, such as IL-1β is upregulated in all examined species, trout TNF-α induce expression of IL-8, IL-17C and cox-2 genes and rock bream HKLs display elevated capability of receptor-mediated phagocytosis upon stimulation with TNF-α (Kim et al., 2009; Li and Zhang, 2016; Zhang et al., 2012; Zou et al., 2003a). In an *in vivo* experiment in tongue sole, elevated levels of IL-1, IL-6, IL-8, IL-27, Toll-like receptor (TLR) 9 and galectin-3-binding protein (G3BP) transcripts were measured in kidney upon injection with a recombinant TNF homologue (Li and Zhang, 2016). Further, Li and Zhang (2016) showed that the receptor binding sites are essential for TNF function, as observed in mammals.

IL-6 has both pro- and anti-inflammatory activities. It was first described as a B cell stimulatory factor, capable of inducing differentiation of B cells to plasma cells and have thereby been linked to antibody production in vertebrates (Hirano et al., 1985, 1986; Kaneda et al., 2012). In mammals IL-6 function as a hepatocyte stimulating factor and a capable inducer of acute phase proteins (Andus et al., 1987; Gauldie et al., 1987).

IL-6 has been identified in several teleosts such as Japanese pufferfish (*Takifugu rubripes*) (Bird et al., 2005), rainbow trout (Iliev et al., 2007), olive flounder (Nam et al., 2007), gilthead seabream (Castellana et al., 2008), zebrafish (Varela et al., 2012), orange-spotted grouper (*Epinephelus coicoides*) (Chen et al., 2012), Atlantic halibut (Øvergard et al., 2012) and Nile tilapia (Wei et al., 2018). These studies report varying tissue expression of IL-6. Studies using conventional PCR reports some absence of IL-6 expression in certain tissues (Castellana et al., 2008; Fujiki et al., 2003; Nam et al., 2007), while later, studies utilizing quantitative PCR reports constitutive expression of IL-6. The relative distribution of IL-6 is highest in lymphoid and central nervous system (CNS) organs, and lowest in liver. In all examined teleosts, IL-6 contains 4 exons and 5 introns.

It has been reported that IL-6 elicits antibody production and regulation of differentiation of naïve T helper (T_h) cells into T_h2 cells *in vivo* in orange-spotted grouper (Chen et al., 2012). The involvement of IL-6 in the promotion of antibody production has also been reported in Nile tilapia (Wei et al., 2018) and Japanese pufferfish (Kaneda et al., 2012). Several works reports IL-6 up-regulation after exposure to pathogens in teleosts; *Streptococcus agalactia* in *in vitro* Nile tilapia, *Edwardisella tarda* in *in vivo* olive founder and *Vibrio anguillarum* in *in vivo* gilthead seabream (Castellana et al., 2008; Nam et al., 2007; Wei et al., 2018). Up-regulation of IL-6 is also observed post stimulation with several PAMPs in teleosts including LPS, bacterial DNA, peptidoglycan, imiquimod and poly (I:C) (Bird et al., 2005; Castellana et al., 2008; Chen et al., 2012; Varela et al., 2012; Wei et al., 2018; Øvergard et al., 2012).

Table 1
Used primers in this study.

Gene	Direction	5′-sequence-3′	Application
RPS20	Forward	GGAGAAGAGCCTGAAGGTGAAG	qPCR
	Reverse	GAGTTTTCCTGGTGGTGATGC	qPCR
IL6	Forward	GAAGACACGCCCACCGACAT	qPCR
	Reverse	GCCCCGCCTGCTCCTCACCT	qPCR
	Forward	GACCGGATGGCTGACGCAA	Sanger sequencing
	Reverse	ACCCAATTTCCACAAGGTAGTGCT	Sanger sequencing
TNFα	Forward	CCACACCACGTTGAGGCAGATCA	qPCR
	Reverse	CCTTGACCGCTTCTCCACTCCA	qPCR
	Forward	GCTGGAAGCACCTGAAGACTCAGACAC	Sanger sequencing
	Reverse	TTGTATCGTGTATGTTACGACCGCATA	Sanger sequencing

Table 2
qPCR assay performance.

Gene	α	Efficiency	R^2	Ampl. size
RPS20	−3299	2,01	0,999	74
IL6	−3398	1,95	0,998	58
TNFα	−3409	1,96	0,996	117

Lumpfish is a representative of the poorly described phylogenetic clade of teleosts, the *Cottales*. Furthermore, it is a novel species for the farming industry in Europe (Powell et al., 2018). The production is successful, but it suffers from high mortality due to bacterial diseases caused by *V. anguillarum*, atypical *Aeromonas salmonicida*, *Pasteurella* sp. and *Pseudomonas anguilliseptica* (Scholz et al., 2018; Walde et al., 2019). Thus, immunological studies in lumpfish is interesting for both phylogenetic, comparative and applied science. In the current study, we have characterized TNF- α and IL-6 in lumpfish. We have examined their tissue - and PAMP dependent gene expression, performed phylogenetic analyses and described their molecular properties.

2. Materials and methods

2.1. Identification of lumpfish (lu) TNF-α and IL-6

In a previous study (Eggestøl et al., 2018) we performed RNA sequencing and *de novo* transcriptome assembly of lumpfish leukocytes, yielding a tri-layered database structure divided into contigs, genes and transcripts. In the current study, we have used this transcriptome as our database to search for TNF-α and IL-6 in lumpfish, and performed a tBLAST-n search utilizing the human TNFα (P01275) and human IL6 (P05231) as our query sequences and chose the top gene ID among the transcript hits. Among that gene ID, we performed a BLAST-X search on all its transcripts against NCBI's non-redundant database and chose the transcript ID with the highest BLAST score among the full-length sequences. Sanger sequencing (see 2.3) verified the sequences.

2.2. Bioinformatical analyses

The phylogenetic analyses included, in addition to the luTNF-α and luIL-6 sequences, all annotated teleost TNF-α and IL-6 sequences in INSDC (Karsch-Mizrachi et al., 2018), human and mouse sequences, and the top 100 hits of a tBLAST-n searches against INSDC's non-

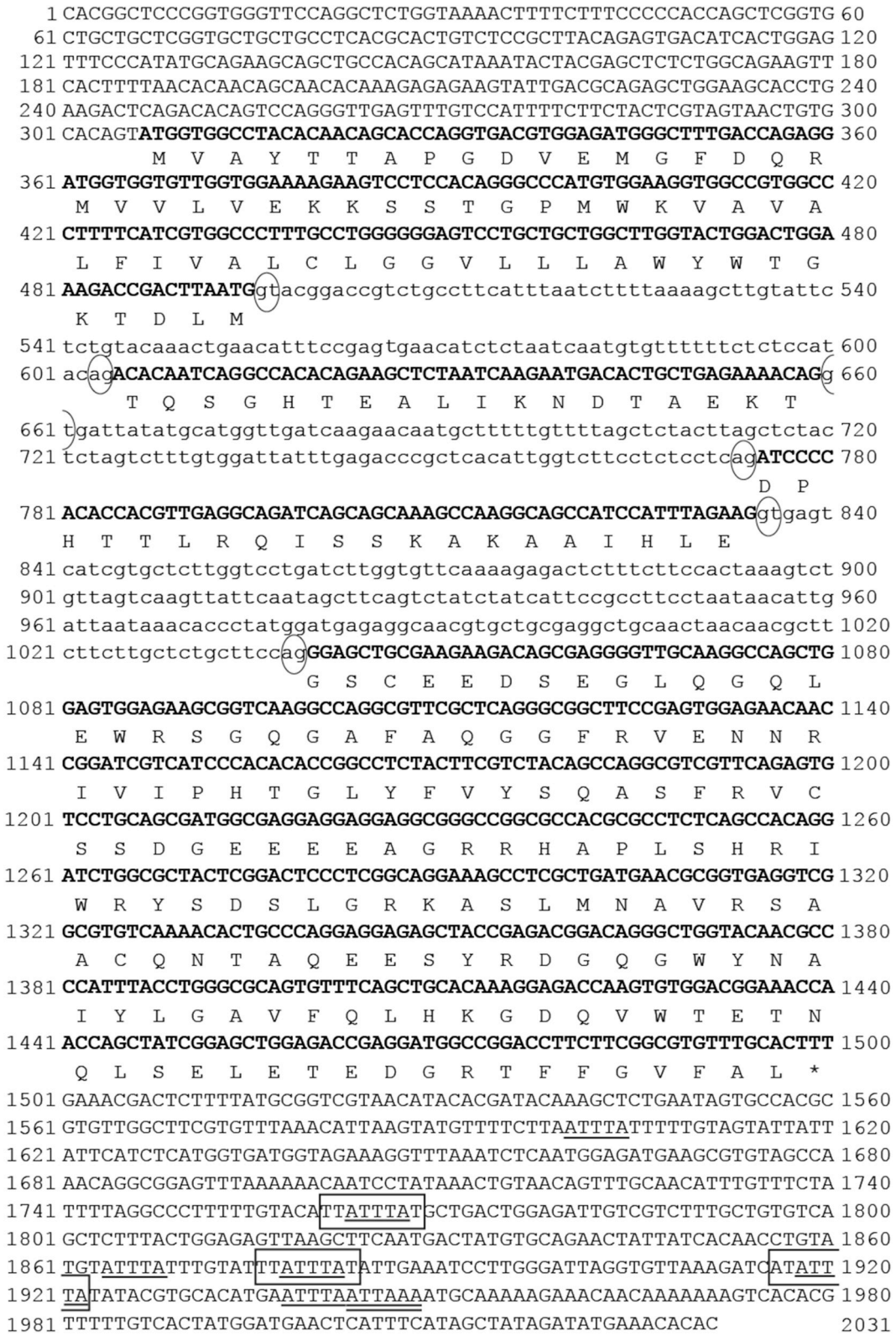

Fig. 1. Nucleotide and deduced amino acid sequences for lumpfish TNF-α. gDNA specific sequence is represented with lower case, cDNA sequence is represented with upper case and coding cDNA sequence is represented with bold. Introns are indicated by ellipses at both ends, AT rich elements are indicated by underlining, double underlining indicates the polyadenylation signal, and the endotoxin responsive motifs are boxed.

redundant database using the lumpfish and zebrafish sequences as queries. In addition for TNF-α, the top 100 hits of a tBLAST-n searches against INSDC's non-redundant database using the Arctic char (*Salvelinus alpinus*) sequences as queries. A preliminary MUSCLE (Edgar, 2004) multiple sequence alignment (MSA) was conducted in order to identify and remove duplicate or inadequate (low quality, partial etc.) sequences, yielding 178 TNF-α and 80 IL-6 sequences for the phylogenetic analyses. Based on these sequences a MUSCLE MSA was made

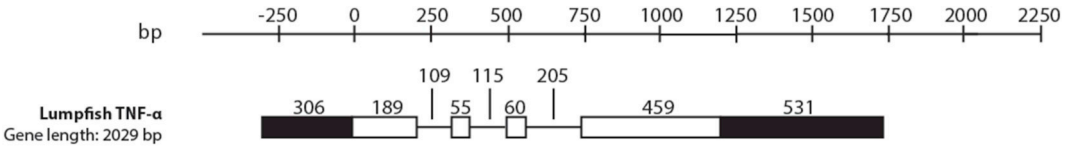

Fig. 2. Genomic organization of lumpfish TNF-α. The zero point is defined as start of peptide coding DNA sequence (CDS). Black boxes represent UTRs, white boxes represents exons and lines represents introns. Numbers represents the number of nucleotides of the corresponding element and parenthesized numbers represent the gene length.

and a maximum likelihood phylogenetic tree utilizing IQ-TREE (Nguyen et al., 2015) with automatic model selection (Kalyaanamoorthy et al., 2017) was constructed (Figs. 7 and 8 and Supplementary Figs. S1 and S2). Bootstrapping was conducted with 100 000 replicates to assess clade support (Minh et al., 2013).

In order to compare the predicted amino acid sequence of luTNF-α and luIL-6 and to identify conserved regions, a MSA was made using the CLUSTALΩ algorithm (Sievers and Higgins, 2014) in which the lumpfish sequences were compared with TNF-α and IL-6 from all teleost sequences fully characterized in the published scientific literature, in addition to human and mouse sequences. In addition, for IL-6, the Tanaka's snailfish (*Liparis tanakae*) sequence were added. Identification of the functional domains was performed by InterProScan (Jones et al., 2014), using the entries from the SMART database (Letunic and Bork, 2018), with the following exceptions: TMHMM used for transmembrane prediction (http://www.cbs.dtu.dk/services/TMHMM/), SignalP-5.0 for signal peptide prediction (http://www.cbs.dtu.dk/services/SignalP-5.0/) and Peptide Cutter for enzyme cleavage site prediction (https://web.expasy.org/peptide_cutter/). Prediction of molecular weight and isoelectric point were performed by ExPASy tool Compute pI/Mw (https://web.expasy.org/compute_pi/).

Scaffolds including luTNF-α and luIL-6 genes, were found by BLAST searching the lumpfish genome with luTNF-α and luIL-6 transcripts in Galaxy (Camacho et al., 2009; Cock et al., 2015; Knutsen, 2018). Intron-exon boundaries were predicted by aligning cDNA and gene sequences and adjusting the introns according to the GT …. AG rule. UTR's were determined by aligning the transcript sequences with the predicted aa sequences.

The tertiary structure of the lumpfish sequences were modeled with SWISS-MODEL (Waterhouse et al., 2018), and fit to murine crystal structures (TNF-α - 2tnf.1.C and IL-6 - 2l3y.1.A). The models and templates were displayed using ICM-Browser 3.8–7b © (MolSoft L.L.C.).

2.3. Sanger sequencing

Sanger sequencing was performed by amplifying the relevant genomic DNA sequence through a high fidelity polymerase chain reaction (PCR) in a 2720 Thermal Cycler (Applied Biosystems, California, USA), using specific primers (Table 1) and Phusion High-Fidelity polymerase (ThermoFischer Scientific) according to the manufactures instructions. The DNA products were extracted from a 1% agarose gel containing GelRed® (Biothium, Fremont, USA). The sequencing reaction was run using the BigDye™ Terminator v3.1 (Applied Biosystems), according to the manufactures instructions and sequenced using the 3730XL Analyzer (Applied Biosystems) at the DNA sequencing Facility at the High-Technology Centre, Bergen, Norway.

2.4. Fish and rearing conditions

Farmed, unvaccinated lumpfish were provided by Vest Aqua base, Norway. The fish were kept at the rearing facilities at the Aquatic and Industrial Laboratory (ILAB), Bergen High-Technology Centre, Bergen, Norway, under normal optimal rearing facilities at a temperature of 8–9 °C, salinity of 34‰ and 12:12 h light:dark. The water flow were 300–400 l per hour and the outlet water had a minimum of 77% oxygen saturation. The fish were fed with commercial dry feed for lumpfish (3 mm pellets).

2.5. Tissue sampling and homogenization

In order to study the normal gene expression in different tissues 16 tissues were collected from fish (n = 7) with an average size of 245.7 ± 49 g and 18.1 ± 1.1 cm,; skin mucus, skin, muscle, thymus, gill filament, gill arch, tongue, liver, spleen, gonad, head kidney (left lobe), heart, pyloric caeca, gut, eye and brain. Up to 40 mg tissue were immediately put in 0.3 ml of fresh lysis buffer in FastPrep® Tubes (MP Biomedicals, USA) containing 3 SS Metal Beads Lysing Matrix (MP Biomedicals, USA) and homogenized in the 24x FastPrep-24™ 5G (MP Biomedicals, USA). Additional 0.4 ml fresh lysis buffer was added after homogenization, according to the manufactures RNA isolation protocol. Isolation of total RNA and cDNA synthesis are described in Section 2.8.

2.6. Leukocyte isolation

For *in vitro* stimulation, leukocytes were isolated from peripheral blood and head kidney from six lumpfish that weighed 282.7 ± 56.5 g and measured 18.5 ± 1.1 cm. The fish were killed by a sharp blow to the head. Leukocytes were isolated from peripheral blood (0.7 ml), collected from *vena caudalis,* as described previously (Haugland et al., 2012). Briefly, the blood was transferred to heparinized containers and diluted to a total volume of 5 ml Leibovitz L-15+ (L-15 media without L-Glutamine adjusted to 370 mOsm by adding 5% (v/v) of a solution consisting of 0.41 M NaCl 0.33 M $NaHCO_3$ and 0.66 5 (w/v) D-glucose) supplemented with 100 μg/ml genatamicin (Lonza Biowhittaker Verviers, Belgium), 10 U/ml heparin (Lonza Biowhittaker Verviers, Belgium) and 15 mM HEPES (Sigma-Aldrich, St. louis, USA)). For isolation of HKL, the anterior 1 cm of the right head kidney lobe was transferred to a gentleMACS™ C tube (Miltenyi Biotec, Germany) containing 3 ml L-15 + medium and dissociated by gentleMACS™ Dissociator (Miltenyi Biotec, Köln, Germany) on the default program D. After dissociation, the cell suspension were placed on discontinuous Percoll gradients, 3 ml 1.070 g/ml Percoll™ (GE Healthcare, Uppsala, Sweden) solution overlaid with 2.5 ml 1.050 g/ml Percoll solution, and centrifuged at 400 g and 4 °C for 40 min. The leukocyte fraction were transferred to a new tube and washed once with L15 + media, centrifuged at 200 g and 4 °C for 10 min, resuspended in L15 + media and counted by CASY® Modell TT cell counter (Innovatis AG, Reutlingen, Germany). All leukocytes samples showed viability over 95% and low levels of aggregation.

2.7. Leukocyte stimulation with PAMPs

Each leukocyte sample in the *in vitro* stimulation experiment was split into eight wells in 24-well plates, each containing 4×10^7 leukocytes and the following PAMPs: 0.3 μg/ml Pam3CSK4 (InvivoGen, San Diego, USA), 0.1 μg/ml FSL-1 (InvivoGen, San Diego, USA), 20 μg/ml Fla-BS (InvivoGen, San Diego, USA), 50 μg/ml poly (I:C) HMW (InvivoGen, San Diego, USA), 10 μg/ml ssPolyU/LyoVec™ (InvivoGen, San Diego, USA), 1 μM CpG-B: T*C*G*T*C*G*T*T*T*T*G*T*C*G*T*T*T*T*G*T*C*G*T*T* (Eurogentech) or 1 μM GpC-B: T*G*C*T*G*C*T*T*T*T*G*T*G*C*T*T*T*T*G*T*G*C*T*T* (Eurogentech), in a total volume of 500 μl of L15 + media. To the non-stimulated control sample, L15 + was added

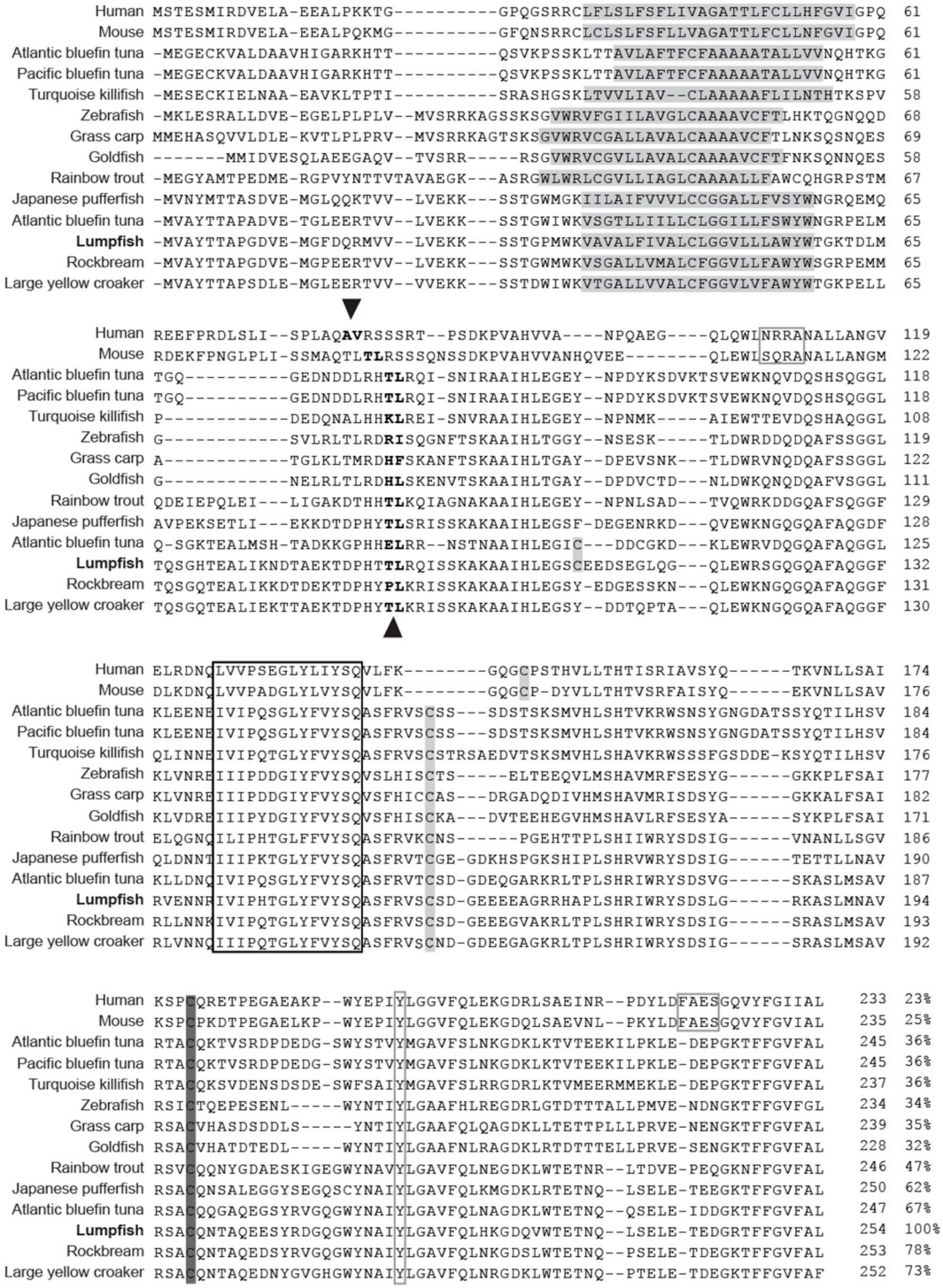

Fig. 3. Multiple alignment of lumpfish TNF-α sequence with other reported teleost, human and murine TNF-α sequences. Cysteine residues is vertically shaded and family signature is boxed in black. Receptor binding surfaces in mammals is boxed in grey. The transmembrane domain is horizontally shaded. The putative TACE cleavage site are in bold type and indicated by arrowheads. Amino acid similarity percentage with lumpfish TNF-α is written as percentage at the end of the respective alignment.

instead of PAMPs. The plates were covered by Microseal® 'B' seal Seals (Bio-Rad, United Kingdom) and incubated at 15 °C. After 18 h, the supernatants were transferred to Eppendorf tubes and centrifuged at 400 g in 10 min at 15 °C. To both the wells and cell pellets 250 µl of lysis solution for total RNA kit (Sigma-Aldrich, St. Louis, USA) were added and subsequently mixed. The lysates were stored at −80 °C.

2.8. Total RNA extraction and cDNA synthesis

Total RNA was isolated using GenElute™ Mammalian Total RNA Miniprep kit (Sigma-Aldrich, St. Louis, USA) according to the manufacturer's instructions and treated by DNase I (up to 2500 ng RNA per reaction) (Sigma-Aldrich, St. Louis, USA) according to the

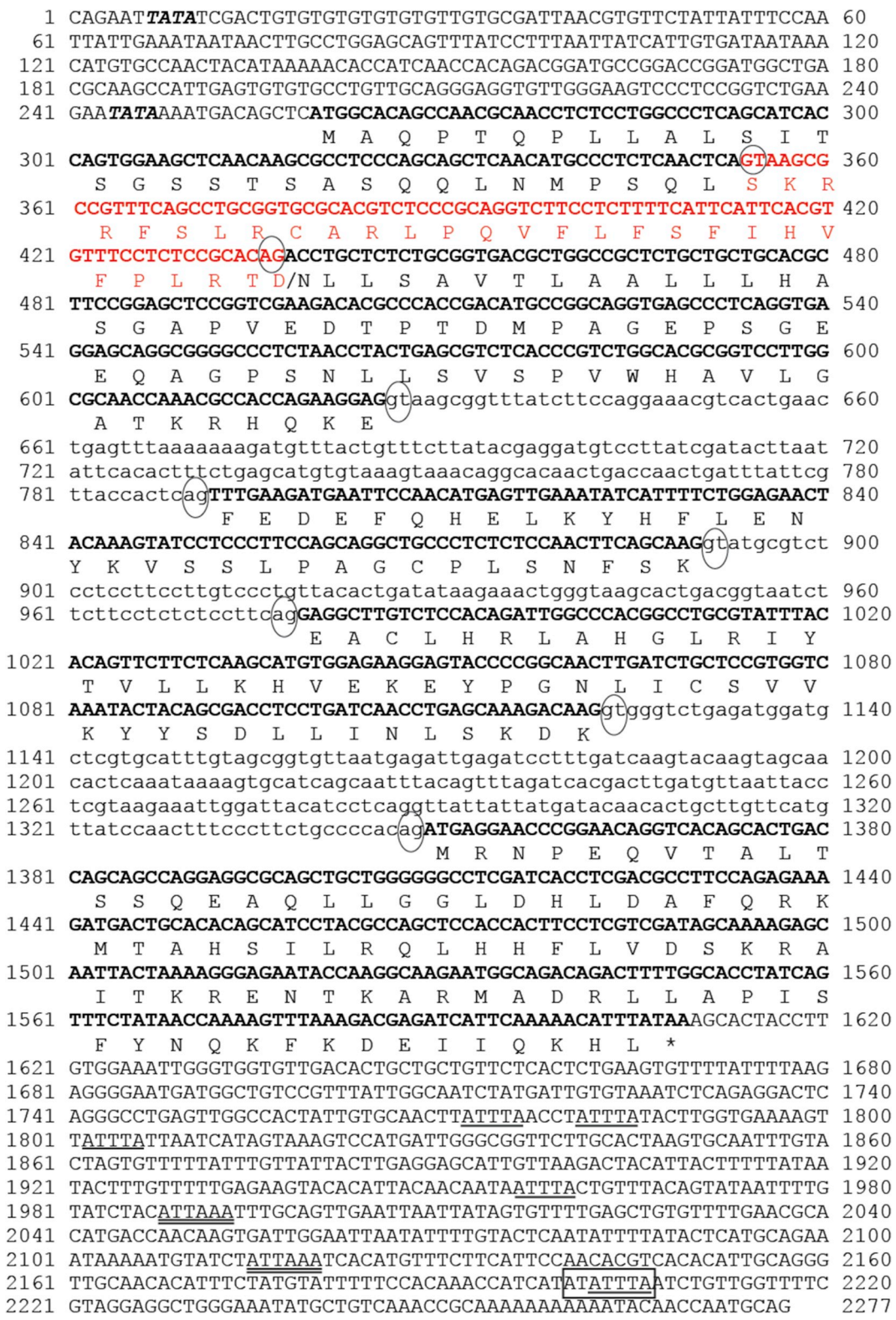

Fig. 4. Nucleotide and deduced amino acid sequences for lumpfish IL-6. gDNA specific sequence is represented with lower case, cDNA sequence is represented with upper case and coding cDNA sequence is represented with bold. Alternatively retained intron are indicated with red letters. Introns are indicated by ellipses at both end, AT rich elements are indicated by underlining, double underlining indicates the polyadenylation signal, the endotoxin responsive motifs are boxed and a TATA box is shown in bold italic. (For interpretation of the references to color in this figure legend, the reader is referred to the Web version of this article.)

manufacturer's instructions. The DNase treated RNA was analyzed on a 1% agarose gel containing GelRed® (Biothium, Fremont, USA) to ensure that all traces of genomic DNA were removed, and to validate the integrity and the quality of the RNA. The RNA concentration and purity was measured in a NanoDrop™ 2000 spectrophotometer (Thermo Fisher Scientific, Waltham, USA). Furthermore, RNA (< 1000 ng/reaction) was reverse-transcribed into cDNA using cDNA synthesis kit (Quantabio, Beverly, USA) according to the manufacturer's instructions.

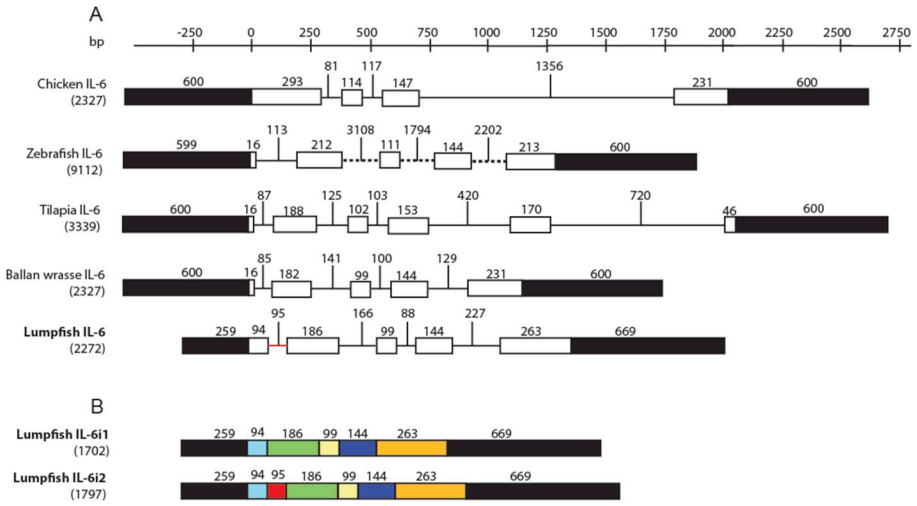

Fig. 5. Genomic organization of IL-6 (A) and transcript organization of luIL-6 (B). The zero point is defined as start of peptide coding DNA sequence (CDS). Black boxes represent UTRs, Numbers represents the number of nucleotides of the corresponding element and parenthesized numbers represent the gene or transcript length. In Fig. 5**A,** white boxes represents exon, black lines represents introns and red lines represents alternatively retained intron. Dashed lines does not correspond with intron length. In Fig. 5**B,** shared exons are represented with same colored boxes, and the alternatively retained intron is represented with a red box. (For interpretation of the references to color in this figure legend, the reader is referred to the Web version of this article.)

2.9. Quantitative PCR (qPCR)

Gene expression were measured by quantitative polymerase chain reaction (qPCR) performed in a C1000 Touch Thermal Cycler with CFX96 Real-Time System (Bio-Rad, Hercules, California) using SYBR Green Jumpstart® Taq DNA Readymix® (Sigma-Aldrich, St. Louis, USA). The pipetting was performed using the PipetMAX 268 (Gilson, Wisconsin, USA). All primers (Table 1) were custom DNA Oligos delivered from Sigma-Aldrich (St. Louis, USA). The target genes assays were optimized for specificity (> 10 000 signal to noise ratio) and efficiency (approximately 2). The performance of the best assay for each gene is reported in Table 2. For relative quantification, the target genes were normalized against the house keeping gene ribosomal protein subunit 20 (RPS20). The qPCR reaction (25 µl) contained 12.5 µl of 2 x SYBR Green Jumpstart® Taq DNA ReadyMix®, 10 µl cDNA (2 ng for RPS20 and 20 ng for target genes), 1 µl (10 µM) of forward and reverse primers and 0.5 µl nuclease-free water (Sigma-Aldrich, St. Louis, USA). The cycling conditions were 94 °C for 5 min followed by 40 cycles of 94 °C for 15 s and 60 °C for 1 min, finishing with a 4 °C hold until termination. For each run, melting curve analyses were performed for each amplicon to ensure the specificity of the primers. Each sample were analyzed by triplicate master mixes. For each master mix a non-template control (NTC) was included to ensure no contamination of the reagents, and a non-reverse transcriptase control (NRT, cDNA reaction without reverse transcriptase) was included to ensure a complete degradation of genomic DNA. For the normal tissue experiment, mean normalized expression (MNE) values were calculated by the ΔCt method (equation (1)), and for the leukocyte stimulation experiment, fold MNE values were calculated by the ΔΔCt method (equation (2)). E is an abbreviation for the assay efficiency, x is any observed Ct value for sample x and y is any observed Ct value for control group sample y.

$$\Delta Ct_x = \frac{E_{target}{}^{-\bar{x}}}{E_{reference}{}^{-\bar{x}}} \quad (1)$$

$$\Delta\Delta Ct_{xy} = \frac{\frac{E_{target}{}^{-\bar{x}}}{E_{reference}{}^{-\bar{x}}}}{\frac{E_{target}{}^{-\bar{y}}}{E_{reference}{}^{-\bar{y}}}} \quad (2)$$

2.10. Statistical analysis

Both qPCR datasets were analyzed by two-way ANOVA in IBM® SPSS® Statistics (version 25.0.0.2) on log10 transformed data. The normal tissue set were followed up by Bonferroni corrected pairwise comparisons and the ligand stimulation set were followed up by Tukey's honest square difference post hoc test. F values refers to the F statistic, df values refers to the degrees of freedom, p values refer to the probability that the statistical summary of the population is equal or more extreme than the observed values of the sample, given that the null hypothesis is true (p values less than 5% is considered significant), and η^2 refers to the effect size, or how much the relevant variable explains the observed variance.

3. Results

3.1. Sequence and structure analysis of luTNF-α and luIL-6

The full-length cDNA sequence of luTNF-α (GenBank accession No: MN093126) composed of 1600 bp with a 5′-untranslated region (UTR) of 306 bp, an open reading frame (ORF) of 762 bp encoding 254 aa and a 3′-UTR of 531 bp containing six AT rich elements, two endotoxin responsive motifs and one polyadenylation signal. The luTNF-α gene was 2031 bp and contained four exons (Figs. 1 and 2). In the translated aa sequence, a transmembrane domain (35–57) and a tumor necrosis factor family domain (96–254) were identified (Fig. 3). Comparative analysis with other TNF-α aa sequences identified a putative TACE cleavage site in luTNF-α (Thr86 and Leu87), resulting in a mature peptide of 168 aa with a theoretic molecular weight of 18.9 kDa and isoelectric point of pH 5.6. Two cysteine residues, known from other species to be involved in the correct folding of the mature peptide, were also present in the luTNF-α. In addition, lumpfish like Atlantic Bluefin tuna contain a cysteine in position 106 and 102, respectively (Fig. 3).

One luIL-6 gene was identified (GenBank accession No: MN093126), having two isoforms. The luIL-6 gene, 2277 bp, contained five exons and four introns (Figs. 4 and 5A). The first exon in luIL-6 is 94 bp (Fig. 5A). This is longer than other non-cyclopteridae/lipridae teleost sequences in which the first exon is typically only 16 bp. The full-length cDNA sequence of the first isoform of luIL-6 (luIL-6 i1) was composed of 1702 bp with a 5′-UTR of 259 bp, an ORF of 775 bp encoding 289 aa and a 3′-UTR of 669 bp containing five AT rich elements, one endotoxin responsive motifs and two polyadenylation signals (Figs. 4 and 5B). The full-length cDNA sequence of the second IL-6 isoform (luIL-6 i2) in lumpfish contained the first intron of the luIL-6 gene, it was composed of 1797 bp, it contained an ORF of 870 bp encoding 289 aa and is a case of alternative intron retention (Figs. 4 and 5B). In the translated aa sequences, the IL-6 family signature sequence were identified. In addition in IL-6 i2, a Caspase 1 cleavage site between position 60 and 61 (DL) (Fig. 6). In the c-termini product a signal peptide sequence were predicted (99.4% probability), but not in the native luIL-6 i2 form (0.6% probability). In IL-6 i1 a signal peptide sequence was predicted with 19% probability. The mature peptides without the predicted signal

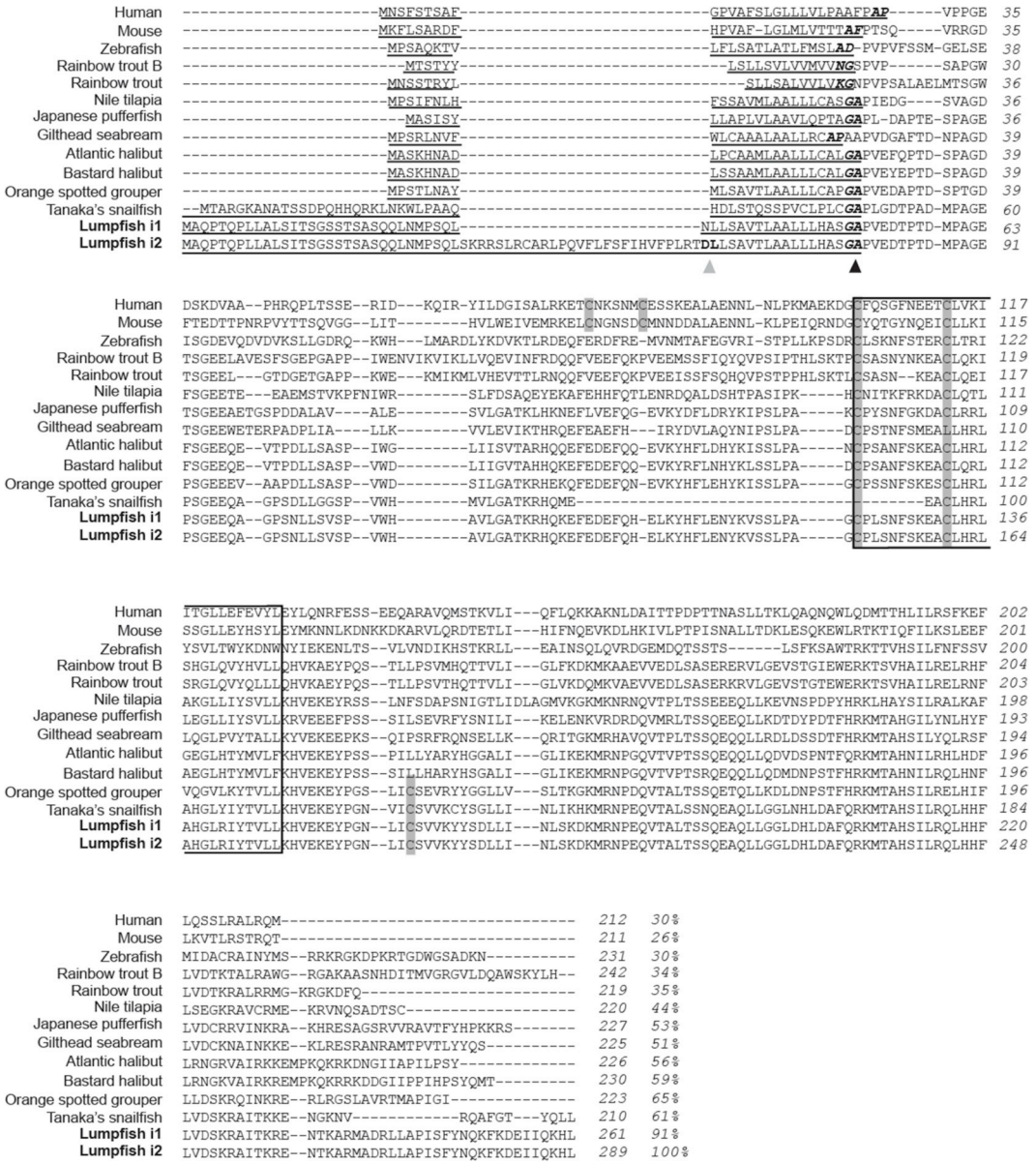

Fig. 6. Multiple alignment of lumpfish IL-6 sequence with other reported teleost, human and murine IL-6 sequences. Cysteine residues are vertically shaded and family signature is boxed in black. Earlier reported and predicted signal peptides is underlined. Putative intron converted aa is horizontally dark grey shaded and UTR converted aa is light grey shaded. Bold letters and grey arrowhead indicate predicted caspase 1 cleavage site. Bold italicized letters and black arrowhead indicate predicted signal peptidase cleavage site. Amino acid similarity percentage with lumpfish IL-6 is written as percentage at the end of the respective alignment.

sequences have a theoretic molecular weight of 24.2 kDa and isoelectric point of pH 7.94. Comparative analysis with other IL-6 sequences revealed that both isoforms of luIL-6 has two conservative cysteine residues. The first cysteine pair in human and mouse are absent in teleosts. Interestingly, 11 positions after the IL-6 family signature sequence, a cysteine residue is present in IL-6 in lumpfish like orange-spotted grouper and Tanaka's snailfish.

3.2. Phylogenetic analysis luTNF-α and luIL-6

The phylogenetic position of luTNF-α was determined through a maximum-likelihood based phylogram (Fig. 7). The teleost TNF-α sequences were divided into three main clades. Clade II contained sequences belonging to *Elopomorpha*, *Osteoglossomorpha* and *Clupeiiformes*, the most basal members of *Teleostei* in this tree. The other teleost sequences were clustered into two clades, corresponding to the TNF-α type-definition proposed for rainbow trout by Hong et al. (2013), clade III and IV. Further, two intra-*Salmonidae* clades of both type I (clade III. a and III. b) and type II (clade IV. a and IV. b) were present, and two intra-*Cyprinae* clades of type II (clade IV. c and IV. d) were also present. LuTNF-α was clustered within the neoteleost clade containing type I TNF-α members (clade III).

The phylogenetic position of luIL-6 was determined through a maximum-likelihood based phylogram (Fig. 8). LuIL-6 was clustered together with other neoteleostei IL-6 sequences. The IL-6 tree reflected the teleost specie tree (clade I, II and III), with the exception of salmoniformes sequences, where two intra-*Salmonidae* clades were present (clade III. a and III. b).

3.3. Homology modelling based structure determination of luTNF-α and IL-6

The structural comparison of luTNF-α monomer with its murine counterpart (Fig. 9) revealed a three-dimensional structure consisting of

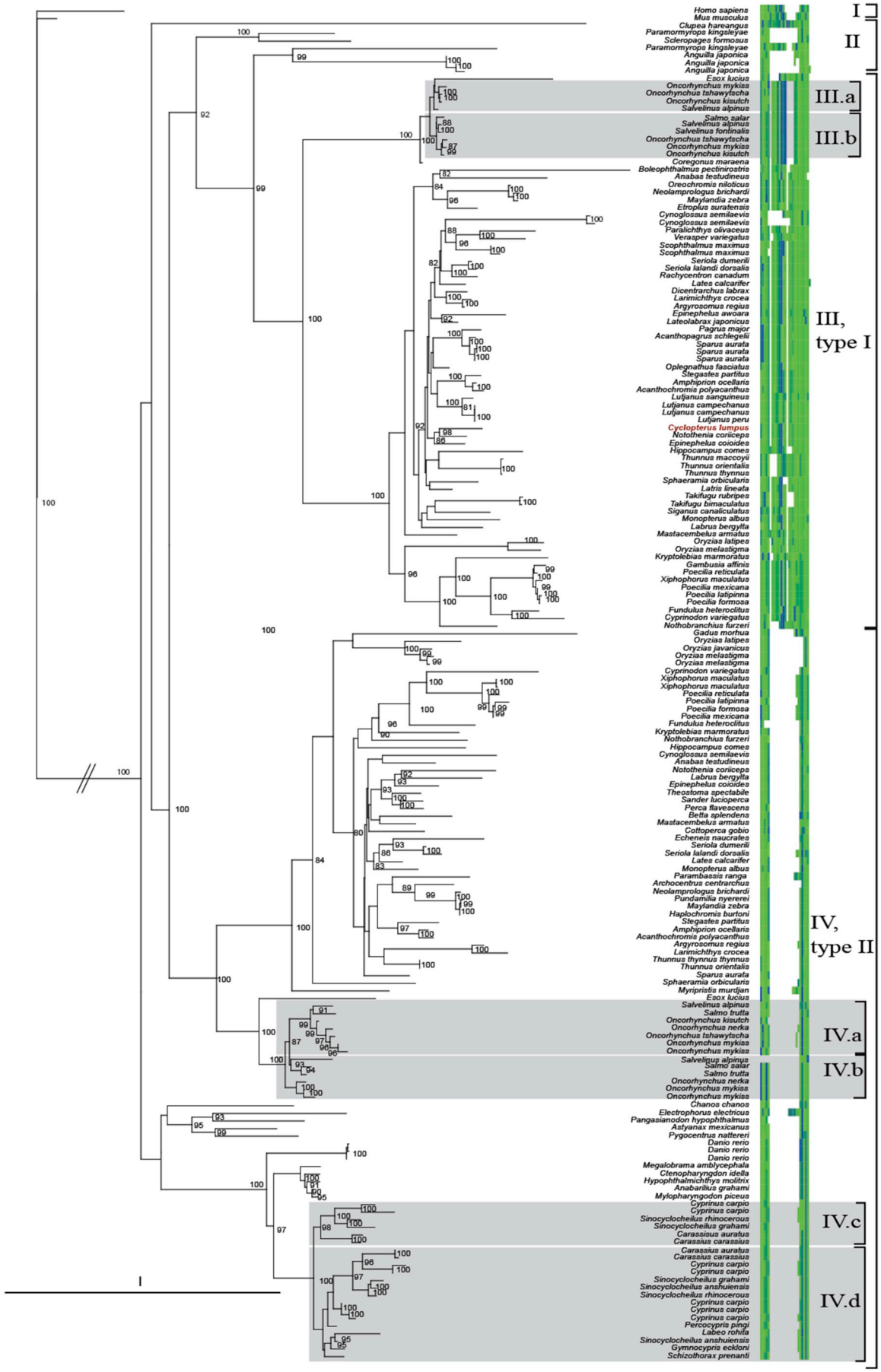

(caption on next page)

Fig. 7. Phylogenetic tree of teleost TNF-α utilizing human and mouse as outgroup. Phylogenetic distance is indicated by branch length and decimal numbers (> 0.1), fat bar indicates distance of 1 amino acid per sequence site. Whole numbers refer to bootstrap values (> 80) of 100000 iterations. Accession numbers are given in the full phylogenetic trees (Supplementary Fig. S1 A, B). Ten clades are indicated by brackets and roman numbers; I – mammalian sequences, II - Elopomorpha, osteoglossomorpha and clupeiiformes sequences, III – type I teleost sequences not present in clade II, IV – type II teleost sequences not present in clade II, V and IV – intra-*Salmonidae* specific type I clades, IIV and IIX – intra-*Salmonidae* specific type II clades, IX and X – intra-*Cyprinidae* specific clades. The intra-clades have been shaded with grey boxes. Alignment defining type affiliation are to the right of the species. Amino acids are colored according to their buried index, dark blue are buried and bright green are not. (For interpretation of the references to color in this figure legend, the reader is referred to the Web version of this article.)

two anti-parallel β-pleated sheets, forming a jellyroll motif, which is the typical protein structure of the TNF-family. LuTNF-α contained a third cysteine residue, only found in lumpfish and Atlantic Bluefin tuna TNF-α1. Due to spatial prediction of this cysteine residue, it is not likely that it contribute in any stabilizing disulfide bridges within the monomer, but it may have a stabilizing function in the trimer, if TNF-α in teleosts have similar quaternary structure as their mammalian counterparts.

The structural comparison of LuIL-6 with its murine counterpart (Fig. 9) showed that LuIL-6 has four conserved α-helices, the typical protein structure of the IL-6 family. LuIL-6 contains a third cysteine residue, presently only found in lumpfish, Tanaka's snailfish and orange spotted grouper IL-6 (Fig. 5). This cysteine residue is placed spatially different from the second cysteine pair known from mammals. The model does not predict the di-sulfide bridge between the first cysteine pair. However, the spatial placement could allow a di-sulfide bridge in luIL-6.

3.4. Gene expression profiling of luTNF- α and luIL-6 in normal tissues

In order to gain insights into the expression of luTNF-α and luIL-6 in different tissues during normal conditions, qPCR assays for luTNF-α and luIL-6 were designed. LuRPS-20 was used as reference gene in a simplex qPCR setup (Fig. 10). Transcripts of all three genes were measured in all examined leukocytes and tissues. A two-way ANOVA showed that TNF-α expression was dependent on tissue ($F(17\ 186) = 8.048$, $p = 5.5E\text{-}16$, $\eta^2 = 0.447$). The highest level of TNF-α transcripts was measured in HKL. It was significantly different from liver, gonad, muscle and gut. The lowest level was measured in gonad and it was significantly different from gill arch, gill filament, HK, heart, HKL, PBL, skin mucus, skin, spleen, thymus and tongue (Fig. 10A). Similar to TNF- α, IL-6 expression was also dependent on tissue ($F(17\ 186) = 8.849$, $p = 1.8E\text{-}16$, $\eta^2 = 0.447$). The highest level of IL-6 transcripts was in brain. It was significantly different from liver, muscle, gut, gill arch, gill filament, gonad, HK, pyloric caeca, skin, skin mucus, tongue. IL6 was expressed at its lowest in gut, being significantly different from brain, eye, gill arch, gill filament, gonad, HK, heart, HKL, PBL, skin, skin mucus, spleen and thymus. (Fig. 10B). A direct comparison showed that the expression level of TNF-α was higher than IL-6 in HKL and all examined organs except brain, eye, gonad and PBL (Fig. 10C). PBL consisted of only two samples due to isolation issues, and therefore should be exempted from questions regarding significance. The statistical analyses showed that there is a significant effect of both tissue and gene $F(17, 186) = 4.278$, $p = 2.5E\text{-}7$, $\eta^2 = 0.281$.

3.5. Modulation of luTNF-α and luIL-6 expression upon exposure to different PAMPs

To further our knowledge of luTNF- α and luIL-6, we stimulated HKL with seven different ligands (Fig. 11). In general, luIL-6 induction was higher than luTNF-α and flagellin was the most potent inducer of luTNF-α resulting in 16.8 times upregulation ($p = 3.12E\text{-}15$) and luIL-6 at 91.8 upregulation ($p = 1.65E\text{-}7$) compared with the control. LuTNF-α was also significantly positively regulated by CpG ($p = 0.0031$) (Fig. 11A). Although, luIL-6 responded higher than luTNF-α, it varied too much to produce statistically significant results for the more moderate inducers of lumpfish HKLs. The ANOVA analysis showed that the examined PAMPs caused significant changes in the expression of both luTNF-α ($F(7, 64) = 25.463$, $p = 3E\text{-}16$, $\eta^2 = 0.736$) and luIL6 ($F(7, 64) = 9.218$, $p = 9E\text{-}8$, $\eta^2 = 0.500$). Also, there was slightly different induction patterns between the genes ($F(7, 64) = 2.214$, $p = 0.044$, $\eta^2 = 0.195$). Both PAM3CSK4 and poly (I:C) was significant inducers of the average measurement of luTNF-α and luIL-6 expression in HKL (Fig. 11B).

4. Discussion

In this study lumpfish TNF-α and IL-6 were identified and characterized. LuTNF-α exhibited all the hallmark traits of teleost TNF-α including four exons and a TNF signature sequence. In addition to a canonical IL-6 (luIL-6i1) which is similar to IL-6 in other species (Bird et al., 2005; Castellana et al., 2008; Chen et al., 2012; Fujiki et al., 2003; Iliev et al., 2007; Kaneda et al., 2012; Nam et al., 2007; Varela et al., 2012; Wei et al., 2018; Øvergard et al., 2012), an alternative isoform retaining the first intron were identified (luIL-6i2) for the first time in teleost IL-6 sequences. The luIL-6 gene have five exons and four introns, of which intron 1 is alternatively retained in lu-IL6 i2. The first exon in luIL-6 is larger than IL-6 in non-cyclopteidae/lipridae teleosts containing 94 bp while the first exon contains 16 bp commonly (Valera et al. 2012). Further, luIL-6 has a much shorter 5′UTR of 259 bp, while other IL-6 sequences typically have 600 bp (Fig. 5). This suggests that the reading frame have been shifted 78 bp upstream in luIL-6, and a reduction of the 5′UTR have occurred. The close lumpfish relative Tanaka's snailfish also contains an elongated IL-6 n-termini entailing that the elongated exon is a feature shared by *Cyclopteridae* and *Lipridae* (Fig. 6). The alternative isoform contained a potential Caspase 1 cleavage site, and *in sillico* analyses indicated that caspase 1 processing is required to produce a signal peptide containing lu-IL6 i2 form. This may lead to four different functionally fates; I – IL-6 i2 is dysfunctional, II – IL-6 is functional intracellularly, III – IL-6 is functional and secreted independent of the Golgi apparatus, and IV – IL6 i2 is functional and is dependent on caspase 1 processing in order to be secreted. If fate IV is true, the kinetics of luIL-6 would have bimodal distribution where the extracellular levels would fluctuate as a consequence of luIL-I i1 levels, and upon recruitment of the inflammasome the levels would increase as the stores of luIL-6 i2 would be converted to IL-6 that is secretable. These fates should be tested experimentally.

Lu TNF-α and IL-6 contain conserved cysteine residues, as other teleosts, suggesting they have disulfide bridges. In addition, both examined lumpfish genes contains another cysteine residue, shared with a few teleosts.

Teleosts have undergone several WGDs. The first teleost-specific (TS) WGD occurred basally in teleosts approximately 320 million years ago (mya), later a *Salmonidae*-specific (SS) WGD occurred approximately 80 mya and most recently a *cyprinae*-specific (CS) WGD occurred 8 mya, reviewed in Ravi and Venkatesh (2018). These WGD are important events, providing additional genetic raw material to evolution giving rise to novel phenotypes. The most common fate of a duplicated gene by WGD (ohnolog) is non-functionalization through accumulation of deleterious mutations. The alternative to non-functionalization is gene retention. Gene retention can take two forms: sub-functionalization; the splitting of original functions and dividing them between the ohnologs, or neo-funtionalization; one ohnolog retains the original functions while the other adopts innovative functions. Species radiated post SS-WGD have probably retained approximately 50% of their

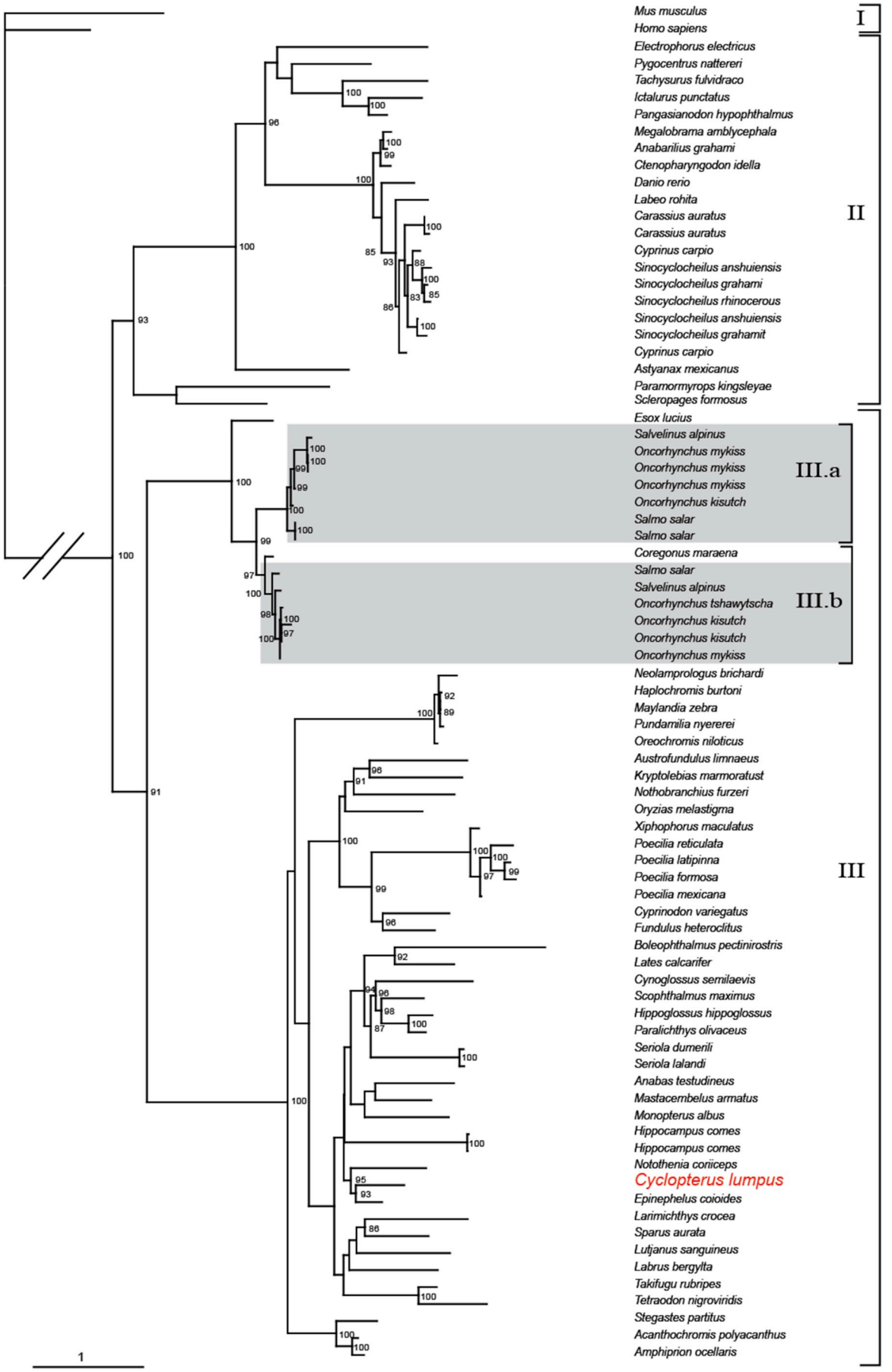

(caption on next page)

Fig. 8. Phylogenetic tree of teleost IL-6 amino acid sequences, utilizing human and mouse as outgroup. Phylogenetic distance is indicated by branch length and decimal numbers (> 0.1), fat bar indicates distance of 1 amino acid per sequence site. Whole numbers refer to bootstrap values (> 80) of 100000 iterations. Accession numbers are given in the full phylogenetic trees (Supplementary Fig. S2). Five clades are indicated by brackets and roman numbers; I – mammalian sequences, II - Elopomorpha, osteoglossomorpha and otomorpha sequences, III – euteleostomorpha sequences, IV and V – intra-*Salmonidae* specific clades. The intra-clades have been shaded with grey boxes.

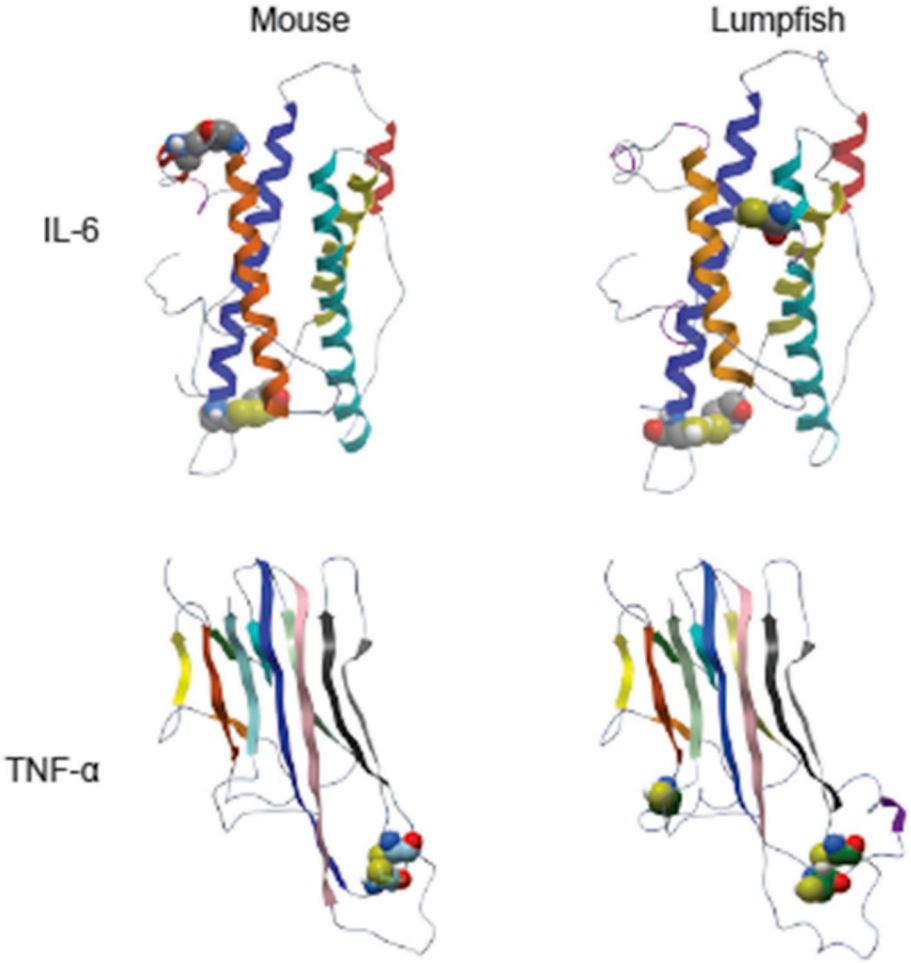

Fig. 9. Tertiary structure models of lumpfish TNF-α and IL-6 peptide sequences using murine templates (respectively: 2tnf.1.C and 2l3y.1.A). α-Helices, β-sheets and sidechain atoms of cysteine residues are varyingly colored, the peptide backbone are in colored in grey.

duplicated genes (Allendorf, 1978), unsurprisingly this have effects in the phylogeny of both TNF-α and IL-6. For IL-6 we observed two intra-*Salmonidae* clades (clade III. a and III. b in Fig. 8) and for TNF-α we observed four intra-*Salmonidae* clades, distributed evenly between one type I clade (clade III. a and III. b in Fig. 7) and one type II clade (clade IV. a and IV. b in Fig. 7) according to the definition by Kadowaki et al. (2009). Due to the members present in both clades, these splits likely rose from the SS-WGD. The IL-6 *Salmonidae* clades are the first evidence of the existence of two IL-6 paralogs within *Salmoniformes*. We also identified two intra-*Cyprinae* clades for TNF-α (clade IV. c and IV. d in Fig. 7). Due to the members present in both clades, it is likely rising from the CS-WGD. Moreover regarding TNF-α, we also observed that all teleosts not belonging to *Elopomorpha*, *Osteoglossomorpha* and *Clupeiiformes* were divided into two clades (clade III and IV in Fig. 7) according to the type affiliation defined by Kadowaki et al. (2009). It is likely that this occurred because of the TS-WGD. The fate of these paralogs had likely not been resolved before the first species were delineated, explaining the more random type affiliation of clade II in Fig. 7. According to the functional suggestion made by Hong et al. (2013) regarding the function of type II TNF-α: "The fish type-II TNF-α has a short stalk that may impact on its enzymatic release or restrict it to a membrane-bound form", the members of clade IV may not function, or have a reduced activity, as a secreted pro-inflammatory cytokine. Highly interestingly all sequences belonging to *Ostariophysi* are exclusively type II TNF-α. This may have profound consequences for the TNF-α biology of the popular model-organism zebrafish and the most important aquaculture species – the cyprinids – of which 44.7 million tonnes were produced in 2017, at a value of 98 billion USD (FAO, 2019).

As expected for important immune genes, both TNF-α and IL-6 is highly expressed in immune organs such as kidney, spleen, thymus and PBL, in lumpfish and other studied teleosts (reviewed Zou and Secombes (2016) and Secombes et al. (2016)). An association of high IL-6 levels and neurological tissues were also observed in lumpfish, as the highest IL-6 expressing organs were brain and eye. High IL-6 levels in brain is also reported from Atlantic halibut (Øvergard et al., 2012). Interestingly, the liver during normal conditions has been identified in several papers as a low TNF-α and IL-6 expressing organ in teleosts. This might be due to the liver being a central vascular organ, and high levels of pro-inflammatory cytokines are known to cause chronical disease. This position is supported by our study as liver was the lowest expressing organ for both genes. In general luTNF-α was significantly

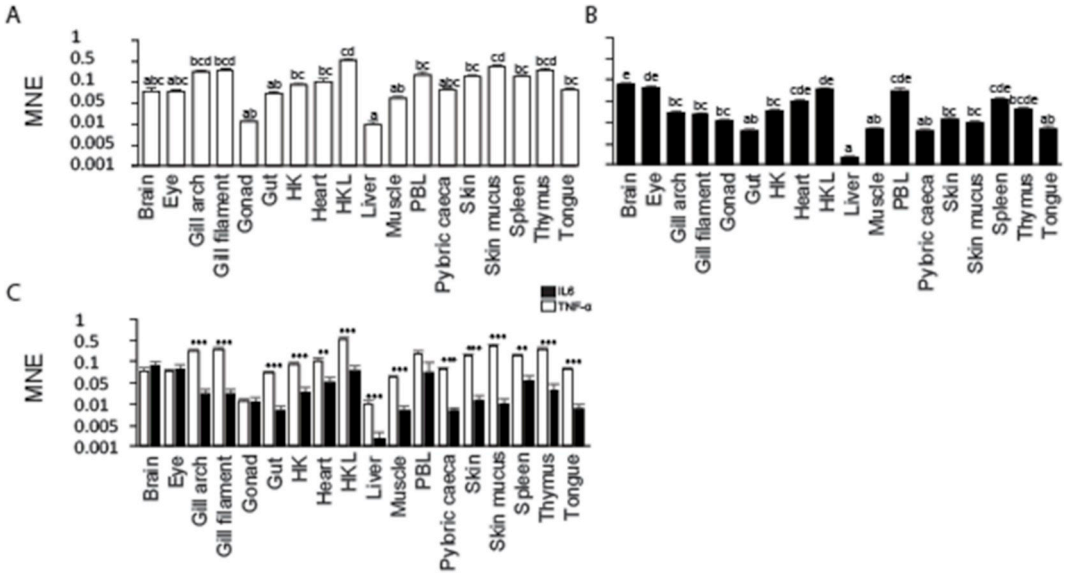

Fig. 10. Tissue distribution of relative expression of luTNF-α and luIL-6 to luRPS20. All data are log10-transfomed in advance of plotting. Error bars denote 1 standard error of the mean (SEM). Differing letters above bars denotes a significant relationship (Bonferroni corrected α-level = 0.05). Full name of abbreviated tissues: HK – Head Kidney, HKL – Head Kidney Leucocytes and PBL – Peripheral Blood Leococytes. **A.** Tissue distribution of IL-6. **B.** Tissue distribution of TNF-α. **C.** Comparison of genes within each tissue. Stars denotes significant comparisons (*p > 0.05, **P > 0.01, ***p > 0.001).

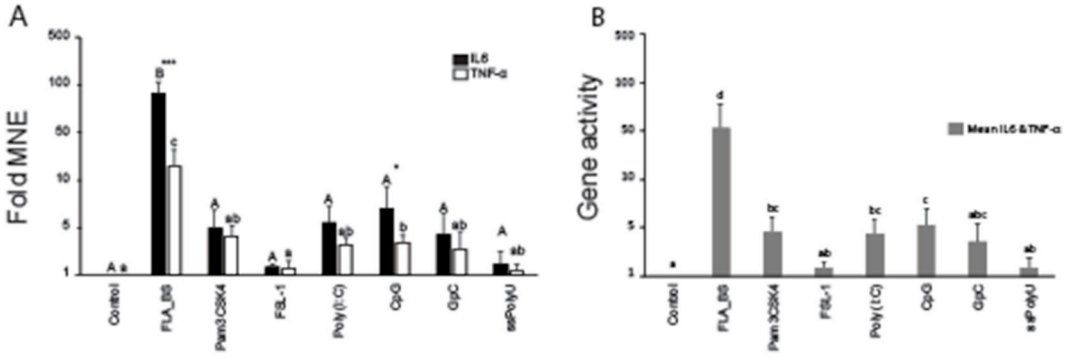

Fig. 11. TNF-α and IL-6 stimulated gene expression post PAMP stimulation in HKLs. All data are log10-transformed in advance of plotting. Error bars denote 1 standard error of the mean (SEM). Differing letters above bars denotes a significant relationship (Bonferroni corrected α-level = 0.05) between PAMPs. **A.** Gene separated PAMP stimulation. Uppercase letters denote TNF-α dependent, lowercase letters denote IL-6 dependent significant relationship between different PAMPs. Stars denotes significant comparisons between genes with the same PAMP treatment (*p > 0.05, **P > 0.01, ***p > 0.001). **B.** PAMP inducible gene activity, in terms of average TNF-α and IL-6 expression.

higher expressed than luIL-6, with the exception of the brain, eye and gonad, suggesting a strong tissue preference of some high TNF-α and/or IL-6 expressing cells or some tissue dependent regulation mechanisms. Moreover, regarding IL-6, several studies have shown high level of IL-6 transcripts in the teleost brain. Øvergard et al. (2012) reported the highest abundance of IL-6 transcripts in the brain, and Varela et al. (2012) revealed a clear appearance of IL-6 transcripts in neuromasts and suggested a role for IL-6 in neurogenesis in zebrafish (Wei et al., 2018). In addition to high expression in immune organs, luTNF-α was also highly expressed in epithelial organs such as; gill, ILT, skin and skin mucus, perhaps reflecting a higher concentration of TNF-α^+ sentinel immune cells in these organs. IL-6 was more potently stimulated than TNF-α, however IL-6 was expressed in a more varyingly manner. These data underpin the known IL-6 behavior; causing more complex downstream effects than TNF-α. Both genes were highly affected by the tested PAMPs.

Knowledge of pro-inflammatory cytokines and innate immunity in lumpfish is interesting from both a comparative and applied perspective. In the current study, we have identified and characterized TNF-α and IL-6 in lumpfish. Since both genes were highly affected by the tested PAMPs, our study suggests that functional feed containing immune stimulants may be an effective prophylactic measure against bacterial and viral diseases in lumpfish. Our analyses form an important basis for further functional analyses and the qPCR assays are valuable to measure effect of immunostimulation and early immune responses in lumpfish. Lumpfish is a novel and economically important species for the farming industry due to its use as cleaner fish. However high mortality caused by bacterial infections is a severe problem. Therefore, to further our understanding of the host-pathogen interactions and the immune system in lumpfish is of major importance.

Acknowledgement

We want to thank Mark M. Powell for valuable discussion about the statistical analyses. The project has been financed by the Research Council in Norway (grant 244148/E40, GTH) and the Univeristy of Bergen.

Appendix A. Supplementary data

Supplementary data to this article can be found online at https://doi.org/10.1016/j.dci.2020.103608.

References

Allendorf, F.W., 1978. Protein polymorphism and the rate of loss of duplicate gene expression. Nature 272, 76–78. https://doi.org/10.1038/272076a0.

Andus, T., Geiger, T., Hirano, T., Northoff, H., Ganter, U., Bauer, J., Kishimoto, T., Heinrich, P.C., 1987. Recombinant human B cell stimulatory factor 2 (BSF-2/IFN-beta 2) regulates beta-fibrinogen and albumin mRNA levels in Fao-9 cells. FEBS Lett. 221, 18–22. https://doi.org/10.1016/0014-5793(87)80344-7.

Baeyens, K.J., De Bondt, H.L., Raeymaekers, A., Fiers, W., De Ranter, C.J., 1999. The structure of mouse tumour-necrosis factor at 1.4 A resolution: towards modulation of its selectivity and trimerization. Acta Crystallogr. Sect. D Biol. Crystallogr. 55, 772–778. https://doi.org/10.1107/s0907444998018435.

Bird, S., Zou, J., Savan, R., Kono, T., Sakai, M., Woo, J., Secombes, C., 2005. Characterisation and expression analysis of an interleukin 6 homologue in the Japanese pufferfish, *Fugu rubripes*. Dev. Comp. Immunol. 29, 775–789. https://doi.org/10.1016/j.dci.2005.01.002.

Bobe, J., Goetz, F.W., 2001. Molecular cloning and expression of a TNF receptor and two TNF ligands in the fish ovary. Comp. Biochem. Physiol. B Biochem. Mol. Biol. 129, 475–481. https://doi.org/10.1016/S1096-4959(01)00353-0.

Camacho, C., Coulouris, G., Avagyan, V., Ma, N., Papadopoulos, J., Bealer, K., Madden, T.L., 2009. BLAST+: architecture and applications. BMC Bioinf. 10, 421. https://doi.org/10.1186/1471-2105-10-421.

Castellana, B., Iliev, D.B., Sepulcre, M.P., Mackenzie, S., Goetz, F.W., Mulero, V., Planas, J.V., 2008. Molecular characterization of interleukin-6 in the gilthead seabream (*Sparus aurata*). Mol. Immunol. 45, 3363–3370. https://doi.org/10.1016/j.molimm.2008.04.012.

Chen, H.H., Lin, H.T., Foung, Y.F., Han-You Lin, J., 2012. The bioactivity of teleost IL-6: IL-6 protein in orange-spotted grouper (*Epinephelus coioides*) induces Th2 cell differentiation pathway and antibody production. Dev. Comp. Immunol. 38, 285–294. https://doi.org/10.1016/j.dci.2012.06.013.

Cock, P.J., Chilton, J.M., Gruning, B., Johnson, J.E., Soranzo, N., 2015. NCBI BLAST+ integrated into Galaxy. GigaScience 4, 39. https://doi.org/10.1186/s13742-015-0080-7.

Dubravec, D.B., Spriggs, D.R., Mannick, J.A., Rodrick, M.L., 1990. Circulating human peripheral blood granulocytes synthesize and secrete tumor necrosis factor alpha. Proc. Natl. Acad. Sci. U.S.A. 87, 6758–6761. https://doi.org/10.1073/pnas.87.17.6758.

Edgar, R.C., 2004. MUSCLE: a multiple sequence alignment method with reduced time and space complexity. BMC Bioinf. 5, 113. https://doi.org/10.1186/1471-2105-5-113.

Eggestøl, H.Ø., Lunde, H.S., Rønneseth, A., Fredman, D., Petersen, K., Mishra, C.K., Furmanek, T., Colquhoun, D.J., Wergeland, H.I., Haugland, G.T., 2018. Transcriptome-wide mapping of signaling pathways and early immune responses in lumpfish leukocytes upon in vitro bacterial exposure. Sci. Rep. 8, 5261. https://doi.org/10.1038/s41598-018-23667-x.

Eimon, P.M., Kratz, E., Varfolomeev, E., Hymowitz, S.G., Stern, H., Zha, J., Ashkenazi, A., 2006. Delineation of the cell-extrinsic apoptosis pathway in the zebrafish. Cell Death Differ. 13, 1619–1630. https://doi.org/10.1038/sj.cdd.4402015.

Fisheries and aquaculture software, 2019. FishStatJ - Software for Fishery and Aquaculture Statistical Time Series. http://www.fao.org/fishery/statistics/global-aquaculture-production/en, Accessed date: 15 November 2019.

Fujiki, K., Nakao, M., Dixon, B., 2003. Molecular cloning and characterisation of a carp (*Cyprinus carpio*) cytokine-like cDNA that shares sequence similarity with IL-6 subfamily cytokines CNTF, OSM and LIF. Dev. Comp. Immunol. 27, 127–136. https://doi.org/10.1016/S0145-305x(02)00074-5.

Garcia-Castillo, J., Pelegrin, P., Mulero, V., Meseguer, J., 2002. Molecular cloning and expression analysis of tumor necrosis factor alpha from a marine fish reveal its constitutive expression and ubiquitous nature. Immunogenetics 54, 200–207. https://doi.org/10.1007/s00251-002-0451-y.

Gauldie, J., Richards, C., Harnish, D., Lansdorp, P., Baumann, H., 1987. Interferon beta 2/B-cell stimulatory factor type 2 shares identity with monocyte-derived hepatocyte-stimulating factor and regulates the major acute phase protein response in liver cells. Proc. Natl. Acad. Sci. U.S.A. 84, 7251–7255. https://doi.org/10.1073/pnas.84.20.7251.

Grayfer, L., Walsh, J.G., Belosevic, M., 2008. Characterization and functional analysis of goldfish (*Carassius auratus* L.) tumor necrosis factor-alpha. Dev. Comp. Immunol. 32, 532–543. https://doi.org/10.1016/j.dci.2007.09.009.

Haugland, G.T., Jakobsen, R.A., Vestvik, N., Ulven, K., Stokka, L., Wergeland, H.I., 2012. Phagocytosis and respiratory burst activity in lumpsucker (Cyclopterus lumpus L.) leucocytes analysed by flow cytometry. PLoS One 7, e47909. https://doi.org/10.1371/journal.pone.0047909.

Hirano, T., Taga, T., Nakano, N., Yasukawa, K., Kashiwamura, S., Shimizu, K., Nakajima, K., Pyun, K.H., Kishimoto, T., 1985. Purification to homogeneity and characterization of human B-cell differentiation factor (BCDF or BSFp-2). Proc. Natl. Acad. Sci. U.S.A. 82, 5490–5494. https://doi.org/10.1073/pnas.82.16.5490.

Hirano, T., Yasukawa, K., Harada, H., Taga, T., Watanabe, Y., Matsuda, T., Kashiwamura, S., Nakajima, K., Koyama, K., Iwamatsu, A., et al., 1986. Complementary DNA for a novel human interleukin (BSF-2) that induces B lymphocytes to produce immunoglobulin. Nature 324, 73–76. https://doi.org/10.1038/324073a0.

Hirono, I., Nam, B.H., Kurobe, T., Aoki, T., 2000. Molecular cloning, characterization, and expression of TNF cDNA and gene from Japanese flounder *Paralychthys olivaceus*. J. Immunol. 165, 4423–4427. https://doi.org/10.4049/jimmunol.165.8.4423.

Hong, S., Li, R., Xu, Q., Secombes, C.J., Wang, T., 2013. Two types of TNF-alpha exist in teleost fish: phylogeny, expression, and bioactivity analysis of type-II TNF-alpha3 in rainbow trout *Oncorhynchus mykiss*. J. Immunol. 191, 5959–5972. https://doi.org/10.4049/jimmunol.1301584.

Hu, W., Wu, W., Sun, S., Liu, Z., Li, A., Gao, L., Liu, X., Liu, D., Deng, H., Zhao, B., Liu, B., Pang, Q., 2019. Identification and characterization of a TNF receptor-associated factor in *Dugesia japonica*. Gene 681, 52–61. https://doi.org/10.1016/j.gene.2018.09.038.

Iliev, D.B., Castellana, B., Mackenzie, S., Planas, J.V., Goetz, F.W., 2007. Cloning and expression analysis of an IL-6 homolog in rainbow trout (*Oncorhynchus mykiss*). Mol. Immunol. 44, 1803–1807. https://doi.org/10.1016/j.molimm.2006.07.297.

Jones, P., Binns, D., Chang, H.Y., Fraser, M., Li, W., Mcanulla, C., Mcwilliam, H., Maslen, J., Mitchell, A., Nuka, G., Pesseat, S., Quinn, A.F., Sangrador-Vegas, A., Scheremetjew, M., Yong, S.Y., Lopez, R., Hunter, S., 2014. InterProScan 5: genome-scale protein function classification. Bioinformatics 30, 1236–1240. https://doi.org/10.1093/bioinformatics/btu031.

Kadowaki, T., Harada, H., Sawada, Y., Kohchi, C., Soma, G., Takahashi, Y., Inagawa, H., 2009. Two types of tumor necrosis factor-alpha in bluefin tuna (*Thunnus orientalis*) genes: molecular cloning and expression profile in response to several immunological stimulants. Fish Shellfish Immunol. 27, 585–594. https://doi.org/10.1016/j.fsi.2008.12.006.

Kalyaanamoorthy, S., Minh, B.Q., Wong, T.K.F., Von Haeseler, A., Jermiin, L.S., 2017. ModelFinder: fast model selection for accurate phylogenetic estimates. Nat. Methods 14, 587–589. https://doi.org/10.1038/nmeth.4285.

Kaneda, M., Odaka, T., Suetake, H., Tahara, D., Miyadai, T., 2012. Teleost IL-6 promotes antibody production through STAT3 signaling via IL-6R and gp130. Dev. Comp. Immunol. 38, 224–231. https://doi.org/10.1016/j.dci.2012.02.002.

Karsch-Mizrachi, I., Takagi, T., Cochrane, G., 2018. The international nucleotide sequence database collaboration. Nucleic Acids Res. 46, D48–D51. https://doi.org/10.1093/nar/gkx1097.

Kim, M.S., Hwang, Y.J., Yoon, K.J., Zenke, K., Nam, Y.K., Kim, S.K., Kim, K.H., 2009. Molecular cloning of rock bream (*Oplegnathus fasciatus*) tumor necrosis factor-alpha and its effect on the respiratory burst activity of phagocytes. Fish Shellfish Immunol. 27, 618–624. https://doi.org/10.1016/j.fsi.2009.07.007.

Knutsen, T.M., 2018. Lumpfish (*Cyclopterus lumpus*) Draft Genome Assembly, Figshare Pubishing Tool. https://doi.org/10.6084/M9.FIGSHARE.7301546.

Krueger, J.M., Fang, J., Taishi, P., Chen, Z., Kushikata, T., Gardi, J., 1998. Sleep. A physiologic role for IL-1 beta and TNF-alpha. Ann. N. Y. Acad. Sci. 856, 148–159. https://doi.org/10.1111/j.1749-6632.1998.tb08323.x.

Laing, K.J., Wang, T., Zou, J., Holland, J., Hong, S., Bols, N., Hirono, I., Aoki, T., Secombes, C.J., 2001. Cloning and expression analysis of rainbow trout *Oncorhynchus mykiss* tumour necrosis factor-alpha. Eur. J. Biochem. 268, 1315–1322. https://doi.org/10.1046/j.1432-1327.2001.01996.x.

Lepen Pleic, I., Secombes, C.J., Bird, S., Mladineo, I., 2014. Characterization of three pro-inflammatory cytokines, TNFalpha1, TNFalpha2 and IL-1beta, in cage-reared Atlantic bluefin tuna *Thunnus thynnus*. Fish Shellfish Immunol. 36, 98–112. https://doi.org/10.1016/j.fsi.2013.10.011.

Letunic, I., Bork, P., 2018. 20 years of the SMART protein domain annotation resource. Nucleic Acids Res. 46, D493–D496. https://doi.org/10.1093/nar/gkx922.

Li, M.F., Zhang, J., 2016. CsTNF1, a teleost tumor necrosis factor that promotes antibacterial and antiviral immune defense in a manner that depends on the conserved receptor binding site. Dev. Comp. Immunol. 55, 65–75. https://doi.org/10.1016/j.dci.2015.10.010.

Li, X., Jia, Z., Wang, W., Wang, L., Liu, Z., Yang, B., Jia, Y., Song, X., Yi, Q., Qiu, L., Song, L., 2017. Glycogen synthase kinase-3 (GSK3) regulates TNF production and haemocyte phagocytosis in the immune response of Chinese mitten crab *Eriocheir sinensis*. Dev. Comp. Immunol. 73, 144–155. https://doi.org/10.1016/j.dci.2017.03.022.

Minh, B.Q., Nguyen, M.A., Von Haeseler, A., 2013. Ultrafast approximation for phylogenetic bootstrap. Mol. Biol. Evol. 30, 1188–1195. https://doi.org/10.1093/molbev/mst024.

Nam, B.H., Byon, J.Y., Kim, Y.O., Park, E.M., Cho, Y.C., Cheong, J., 2007. Molecular cloning and characterisation of the flounder (*Paralichthys olivaceus*) interleukin-6 gene. Fish Shellfish Immunol. 23, 231–236. https://doi.org/10.1016/j.fsi.2006.10.001.

Nguyen, L.T., Schmidt, H.A., Von Haeseler, A., Minh, B.Q., 2015. IQ-TREE: a fast and effective stochastic algorithm for estimating maximum-likelihood phylogenies. Mol. Biol. Evol. 32, 268–274. https://doi.org/10.1093/molbev/msu300.

Ordas, M.C., Costa, M.M., Roca, F.J., Lopez-Castejon, G., Mulero, V., Meseguer, J., Figueras, A., Novoa, B., 2007. Turbot TNFalpha gene: molecular characterization and biological activity of the recombinant protein. Mol. Immunol. 44, 389–400. https://doi.org/10.1016/j.molimm.2006.02.028.

Øvergard, A.C., Nepstad, I., Nerland, A.H., Patel, S., 2012. Characterisation and expression analysis of the Atlantic halibut (*Hippoglossus hippoglossus* L.) cytokines: IL-1beta, IL-6, IL-11, IL-12beta and IFNgamma. Mol. Biol. Rep. 39, 2201–2213. https://doi.org/10.1007/s11033-011-0969-x.

Powell, A., Treasurer, J.W., Pooley, C.L., Keay, A.J., Lloyd, R., Imsland, A.K., Garcia De Leaniz, C., 2018. Use of lumpfish for sea-lice control in salmon farming: challenges and opportunities. Rev. Aquac. 10, 683–702. https://doi.org/10.1111/raq.12194.

Praveen, K., Evans, D.L., Jaso-Friedmann, L., 2006. Constitutive expression of tumor necrosis factor-alpha in cytotoxic cells of teleosts and its role in regulation of cell-mediated cytotoxicity. Mol. Immunol. 43, 279–291. https://doi.org/10.1016/j.molimm.2005.01.012.

Qu, F., Xiang, Z., Zhou, Y., Qin, Y., 2017. A molluscan TNF receptor-associated factor 2 (TRAF2) was involved in host defense against immune challenges. Fish Shellfish Immunol. 71, 105–115. https://doi.org/10.1016/j.fsi.2017.09.076.

Ravi, V., Venkatesh, B., 2018. The divergent genomes of teleosts. Annu. Rev. Anim. Biosci. 6, 47–68. https://doi.org/10.1146/annurev-animal-030117-014821.

Saeij, J.P.J., Stet, R.J.M., De Vries, B.J., Van Muiswinkel, W.B., Wiegertjes, G.F., 2003. Molecular and functional characterization of carp TNF: a link between TNF

polymorphism and trypanotolerance? Dev. Comp. Immunol. 27, 29–41. https://doi.org/10.1016/s0145-305x(02)00064-2.
Savan, R., Sakai, M., 2004. Presence of multiple isoforms of TNF alpha in carp (*Cyprinus carpio* L.): genomic and expression analysis. Fish Shellfish Immunol. 17, 87–94. https://doi.org/10.1016/j.fsi.2003.11.001.
Scholz, F., Glosvik, H., Marcos-Lopez, M., 2018. Cleaner fish health. In: Treasurer, J. (Ed.), Cleaner Fish Biology and Aquaculture Applications. 5M Publishing Ltd., UK, pp. 221–257.
Secombes, C.J., Wang, T., Bird, S., 2016. Vertebrate cytokines and their evolution. In: Malagoli, D. (Ed.), The Evolution of the Immune System. Academic Press, pp. 87–150.
Sievers, F., Higgins, D.G., 2014. Clustal omega. Curr. Protoc. Bioinform. 48, 3. https://doi.org/10.1002/0471250953.bi0313s48. 13.11-13.13.16.
Uenobe, M., Kohchi, C., Yoshioka, N., Yuasa, A., Inagawa, H., Morii, K., Nishizawa, T., Takahashi, Y., Soma, G., 2007. Cloning and characterization of a TNF-like protein of *Plecoglossus altivelis* (ayu fish). Mol. Immunol. 44, 1115–1122. https://doi.org/10.1016/j.molimm.2006.07.281.
Varela, M., Dios, S., Novoa, B., Figueras, A., 2012. Characterisation, expression and ontogeny of interleukin-6 and its receptors in zebrafish (Danio rerio). Dev. Comp. Immunol. 37, 97–106. https://doi.org/10.1016/j.dci.2011.11.004.
Walde, C., Gulla, S., Hansen, H., Mjølnerød, E., Bornø, G., 2019. Fish Health Report 2018. The Health of Cleaner Fish (In Norwegian), vols. 119–125 The Norwegian Veterinary Institute.
Warner, S.J., Libby, P., 1989. Human vascular smooth muscle cells. Target for and source of tumor necrosis factor. J. Immunol. 142, 100–109.
Waterhouse, A., Bertoni, M., Bienert, S., Studer, G., Tauriello, G., Gumienny, R., Heer, F.T., De Beer, T.a.P., Rempfer, C., Bordoli, L., Lepore, R., Schwede, T., 2018. SWISS-MODEL: homology modelling of protein structures and complexes. Nucleic Acids Res. 46, W296–W303. https://doi.org/10.1093/nar/gky427.
Wei, X., Li, B., Wu, L., Yin, X., Zhong, X., Li, Y., Wang, Y., Guo, Z., Ye, J., 2018. Interleukin-6 gets involved in response to bacterial infection and promotes antibody production in Nile tilapia (*Oreochromis niloticus*). Dev. Comp. Immunol. 89, 141–151. https://doi.org/10.1016/j.dci.2018.08.012.
Young, J.D., Liu, C.C., Butler, G., Cohn, Z.A., Galli, S.J., 1987. Identification, purification, and characterization of a mast cell-associated cytolytic factor related to tumor necrosis factor. Proc. Natl. Acad. Sci. U.S.A. 84, 9175–9179. https://doi.org/10.1073/pnas.84.24.9175.
Zhang, A., Chen, D., Wei, H., Du, L., Zhao, T., Wang, X., Zhou, H., 2012. Functional characterization of TNF-alpha in grass carp head kidney leukocytes: induction and involvement in the regulation of NF-kappaB signaling. Fish Shellfish Immunol. 33, 1123–1132. https://doi.org/10.1016/j.fsi.2012.08.029.
Zou, J., Secombes, C.J., 2016. The function of fish cytokines. Biology 5. https://doi.org/10.3390/biology5020023.
Zou, J., Wang, T., Hirono, I., Aoki, T., Inagawa, H., Honda, T., Soma, G.I., Ototake, M., Nakanishi, T., Ellis, A.E., Secombes, C.J., 2002. Differential expression of two tumor necrosis factor genes in rainbow trout, *Oncorhynchus mykiss*. Dev. Comp. Immunol. 26, 161–172. https://doi.org/10.1016/S0145-305X(01)00058-1.
Zou, J., Peddie, S., Scapigliati, G., Zhang, Y., Bols, N.C., Ellis, A.E., Secombes, C.J., 2003a. Functional characterisation of the recombinant tumor necrosis factors in rainbow trout, *Oncorhynchus mykiss*. Dev. Comp. Immunol. 27, 813–822. https://doi.org/10.1016/S0145-305X(03)00077-6.
Zou, J., Secombes, C.J., Long, S., Miller, N., Clem, L.W., Chinchar, V.G., 2003b. Molecular identification and expression analysis of tumor necrosis factor in channel catfish (*Ictalurus punctatus*). Dev. Comp. Immunol. 27, 845–858. https://doi.org/10.1016/S0145-305X(03)00085-5.